IEEE Access
Multidisciplinary : Rapid Review : Open Access Journal

Received July 22, 2020, accepted August 17, 2020, date of publication August 31, 2020, date of current version September 21, 2020.

Digital Object Identifier 10.1109/ACCESS.2020.3020267

A Bayesian Receiver for Semiblind Equalization in Sparse Underwater Acoustic Channels Using Bernoulli Priors

LING WANG, ZHE JIANG, AND HAIYAN WANG, (Member, IEEE)

School of Marine Science and Technology, Northwestern Polytechnical University, Xi'an 710072, China

Corresponding author: Zhe Jiang (jzh1723@nwpu.edu.cn)

This work was supported in part by the NSF of China under Grant 61771401, Grant 61401364, and Grant 61571365, and in part by the National Key Research and Development Program of China under Grant 2016YFC1400200.

ABSTRACT Underwater acoustic channels are characterized by sparse channel structures, where very few significantly strong non-zero taps exist out of long delay spreads. Though some existing works typically have attempted to take advantage of the sparsity of multipath channels, substantial performance improvement remains elusive. In this work, we develop an iterative Markov chain Monte Carlo (MCMC) algorithm based on Gibbs sampling designed for sparse channels. We decompose the sparse channel response into components of sparsity pattern and sparse coefficient, and incorporate the sparse structure of channels in Bernoulli prior probability distribution for sparsity pattern. We derive the posterior distributions of both sparsity pattern and sparse coefficient components, thereby sampling of sparse channels could be obtained. Furthermore, our proposed algorithm is also generalizable to time-varying underwater acoustic channels. Numerical results are provided to demonstrate performance of our proposed algorithm.

INDEX TERMS Semiblind equalization, Gibbs sampling, sparse channels, underwater acoustic communications.

I. INTRODUCTION

The underwater acoustic environment poses significant challenges, such as limited available bandwidth, large delay spread, time-varying multipath propagation and low speed of acoustic waves, etc, to the design of communication systems [1]–[5]. It is quite challenging to communicate over the multipath channel with an excessive delay, which introduces significant intersymbol interference (ISI).

Many underwater acoustic channels have sparse multipath structures in the time domain. Sparse frequency selective channels tend to have long delay spreads but only very few significantly strong non-zero parameters. Taking advantage of channel sparsity could substantially reduce the number of channel parameters for estimation and tracking, thereby substantially lowering the algorithm complexity. Therefore exploiting sparsity nature of underwater acoustic channels to estimate channel or/and detect transmitted symbols has been a hot research topic.

The associate editor coordinating the review of this manuscript and approving it for publication was Xingwang Li.

In [6], the estimation of sparse shallow-water acoustic communication channels based on the delay-Doppler-spread function representation of the channel and the impact of estimation performance on the equalization of phase coherent communication signals were investigated. Reference [7] proposed an adaptive sparse partial response equalizer (SPRE) well matched with the channel characteristics to mitigate the ISI efficiently. [8] studied the practical application of an iterative detection and decoding (IDD) framework to underwater acoustic communications (UAC) by elaborating on channel-estimate-based minimum mean-square error turbo equalization (CE-based MMSE-TEQ) and a direct adaptive turbo equalization (DA-TEQ). The dimensionality of the equalizer is reduced by capturing sparse channel structure. Reference [9] explored frequency-domain oversampling to improve the system performance of zero-padded (ZP) orthogonal frequency division multiplexing (OFDM) transmissions over underwater acoustic channels with large Doppler spread. A signal design that enables the separation between sparse channel estimation and data detection was used to reduce equalization complexity. In [10], the authors investigated the multicarrier transmission in one particular type of underwater acoustic channels, which have extremely long delay spreads but clustered multipath arrivals. A sparse channel estimator by treating the two clusters of the long channel as two virtual quasi-synchronous channels was presented. Reference [11] proposed an algorithmic framework for sparse channel identification and a suit of algorithms by minimizing a differentiable cost function that utilizes the underlying Riemannian structure of the channel as well as the L_0-norm of the complex-valued channel taps. In [12], the authors proposed a gradient-descent approach to refine the channel estimates obtained by standard sparse channel estimators. Reference [13] assumed a feedback link from the receiver with a quantized estimate of the sparse channel impulse response for adaptive modulations. Reference [14] considered a channel parameter estimation problem using a wideband multichannel receiver array and estimated the sparse underwater acoustic communication channel parameters including time-delay, incidence angle, Doppler frequency, and complex amplitude of impinging multipath components. In [15], the authors proposed a two-stage sparse channel estimation technique, which estimated the delay and Doppler scale sequentially, by parameterizing the amplitude variation and delay variation of each path with polynomial approximation. Reference [16] used the improved proportionate normalized least mean squares (IPNLMS) algorithm for iterative channel estimation in turbo equalization by exploiting the sparse nature of underwater acoustic channels. Reference [17] presented a channel-estimate-based decision feedback equalizer (CEB-DFE) that dealt with high platform mobility by exploiting sparse multipath structures. Reference [18] conducted a thorough investigation of preamble detection in adverse underwater acoustic channels in the presence of various external interferences, and proposed two novel detection methods based on the inherent sparsity of underwater acoustic channels. Reference [19] investigated the estimation and prediction of the sparse time-varying channel in underwater acoustic (UWA) systems and proposed an adaptive channel prediction scheme that extrapolated the channel knowledge from a block of training symbols. Reference [20] presented a low complexity frequency domain channel estimator exploiting the channel sparsity.

However, these works did not consider blind/semiblind data reception, which is preferable in bursty communication links from an efficiency point of view [21]. Monte Carlo Markov chain (MCMC) technique has been extensively investigated in wireless communications, and proved to be efficient for joint channel estimation and data detection in a blind manner [22]–[28]. MCMC is recently beginning to make impact on UAC. In specific, the Gibbs sampler technique has been employed as an alternative to the popular matching-pursuit-type algorithms [6], [29]. Chen and Peng [30] proposed an MCMC-based noncoherent UAC reception scheme, whereas in the coherent UAC context MCMC-based detector was used with a separate channel estimation module. In [31], the authors considered a statistical semiblind equalizer implemented by the Gibbs sampler technique. The proposed equalizer conducted channel estimation and symbol detection in a joint manner, and it was robust to the accuracy of the channel information. Nevertheless, these works did not exploit the sparse nature of underwater acoustic channels.

In this work, we focus on the problem of semiblind equalization that deals with sparse underwater acoustic channels. We develop an iterative MCMC algorithm based on Gibbs sampling designed for sparse channels. We decompose the sparse channel response into components of sparsity pattern and sparse coefficient, and incorporate the sparse structure of channels in Bernoulli prior probability distribution for sparsity pattern. We derive the posterior distributions of both sparsity pattern and sparse coefficient components, thereby sampling of sparse channels could be obtained. In principle, the Gibbs-sampler-based equalizer could operate blindly by ignoring the initial channel information. However, the performance of a blind equalizer is vulnerable to the potential problem of phase and shift ambiguities [23]. Therefore, we incorporate rough initial channel information to construct semiblind equalizer as in [31]. Furthermore, our proposed algorithm is also generalizable to non-sparse channels. Although we focus on uncoded UAC systems, the extension to coded UAC systems is straightforward.

We summarize the contributions in this work as follows:

1) Proposal of a new semiblind equalization algorithm based on Gibbs sampling for sparse multipath underwater acoustic channels by using Bernoulli priors. The posterior distributions of both sparsity pattern and sparse coefficient are derived to obtain the proposed algorithm.
2) The semiblind equalization algorithm in both single-carrier (SC) and OFDM communication systems are derived.
3) Numerical results are provided to demonstrate performance of our proposed algorithm, showing that the proposed algorithm outperforms existing algorithms.

The rest of this paper is organized as follows. In Section II, we introduce the system model and problem formulation. In Section III, we present an iterative MCMC algorithm based on Gibbs sampling designed for sparse channels.. We present computer simulation results in Section IC for performance verification before concluding with Section V.

II. SYSTEM MODEL

In this paper, we will consider both SC and OFDM communication systems. For SC systems, denote a block of N transmitting data symbols as $\{x_n\}_{n=0}^{N-1}$, which are assumed to be independently drawn from a finite alphabet set $\mathcal{A} = \{Q_1, Q_2, \ldots, Q_{|\mathcal{A}|}\}$. Let $\{h_l\}_{l=0}^{L}$ stands for the channel impulse response, where the length of channel is $L+1$. The received signals could be represented by the following linear finite impulse response (FIR) model [27]

$$y_n = \sum_{l=0}^{L} h_l x_{n-l} + w_n, \quad n = 0, 1, \ldots, N-1+L \quad (1)$$

where n is the time index; $\{w_n\}_{n=0}^{N-1+L}$ are independent and identically distributed (i.i.d.) complex Gaussian noise samples with zero-mean and a variance of σ^2, and are independent of data symbols $\{x_n\}_{n=0}^{N-1}$. Note that we take the whole received signal samples $\{y_n\}_{n=0}^{L-1+L}$ into consideration due to channel memory. Furthermore, we let $x_{-L} = \cdots = x_{-1} = 0$ and $x_N = \cdots = x_{N-1+L} = 0$ in (1) for notational convenience.

For OFDM systems, denote transmitting data symbols at K subcarriers as $\boldsymbol{x}$, where K is the number of subcarriers. Let $\boldsymbol{h}_0 = [h_1, \ldots, h_L, 0, \ldots, 0]^T$ stands for the channel impulse response in time-domain with extra $K-L$ zeros. The received signals $\boldsymbol{y}_F$ at K subcarriers in frequency-domain are given by [22]

$$\boldsymbol{y}_F = diag\{\boldsymbol{x}\}\boldsymbol{F}\boldsymbol{h}_0 + \boldsymbol{w}_F \quad (2)$$

where $\boldsymbol{w}_F$ is a sequence of i.i.d. complex Gaussian noise samples with zero-mean and a variance of σ^2; $\boldsymbol{F}$ is the $K \times K$ DFT matrix.

Note that we have assumed that the channel remains constant over observed samples in (1) and (2), which is a common assumption to model underwater acoustic channels, e.g., in [6], [11], [16], [32]. For the case of fast channel variations, the parameter of Doppler rate may be introduced to model the time-varying characteristic of underwater acoustic channel such as in [9], [10], [13]. In this case, our algorithm could be adapted by adding an extra step to sample from the posteriori probability density function of Doppler rate.

In this paper, we use Bernoulli-based model to represent channel sparsity. In specific, sparse channel $\boldsymbol{h}$ follows the model [33]

$$\boldsymbol{h} = \boldsymbol{a}_s \odot \boldsymbol{c}_s \quad (3)$$

where $\boldsymbol{a}_s \in \{0, 1\}^L$ is the sparsity pattern, whose entries are drawn i.i.d. from Bernoulli distribution with parameter q ($q \ll 1$), denoted by $B(q)$; $\boldsymbol{c}_s$ stands for the vector of sparse coefficient.

Remark: Note that the sparse structure of $\boldsymbol{h}$ in (3) could be easily removed by specifying q being 1. Therefore, the formulation and corresponding algorithm could be generally applied in nonsparse channels.

III. SEMIBLIND EQUALIZATION IN SPARSE CHANNELS

In this section, we propose a MCMC-based semiblind sparse equalizer, since MCMC algorithm is able to solve nonlinear and high-dimensional problem efficiently. In general, the MCMC equalizer is implemented in two steps. In the first step, the Gibbs sampler generates a collection of sample vectors $\boldsymbol{x}^{(n)}$ and $\boldsymbol{h}^{(n)}$ for $n = 0, 1, \ldots, I$. In the second step, the transmitted symbols (and channel response) are determined from the obtained samples.

A. PRIOR DISTRIBUTIONS FOR SPARSE CHANNELS

Existing works assume a conjugate prior distribution, which is a multivariate normal distribution, or a non-informative distribution for channel $\boldsymbol{h}$. The posteriori distribution of $\boldsymbol{h}$ in either case is a normal distribution with the parameters (mean and variance) updated by the received samples. In this work, we decompose the channel response into components of sparsity pattern and sparse coefficient as in (3), and use Bernoulli distribution for sparsity pattern to promote the sparse structure of the channel prior. In specific, the prior distribution for the ith element of $\boldsymbol{a}_s$ is

$$\begin{cases} p(a_{si} = 1) = q \\ p(a_{si} = 0) = 1 - q \end{cases} \quad (4)$$

for $i = 1, \ldots, L+1$, where q is the hyperparameter which depicts Bernoulli distribution.

For sparse coefficient $\boldsymbol{a}_s$, we use hierachical prior distribution as

$$\begin{cases} p(c_{si}|a_{si} = 0) = \delta(c_{si}) \\ p(c_{si}|a_{si} = 1) = \exp(-c_{si}^2/\sigma_0^2)/\sqrt{2\pi\sigma_0^2} \end{cases} \quad (5)$$

where σ_0^2 is the hyperparameter.

B. GIBBS SAMPLING OF SPARSE CHANNELS

In the framework of Gibbs sampling, we need to derive posterior distributions with respect to unknown parameters. We first derive the posterior distributions for both sparsity pattern and sparse coefficient components, thereby sampling of sparse channels could be obtained.

1) SAMPLING SPARSE CHANNELS IN SC SYSTEMS

To derive the posterior distribution of the channel $\boldsymbol{h}$ for SC systems, define

$$\boldsymbol{X} \triangleq \begin{bmatrix} \boldsymbol{x}_{10} & \cdots & \boldsymbol{x}_{L0} \end{bmatrix} \triangleq \begin{bmatrix} x_1 & & \boldsymbol{0} \\ \vdots & \ddots & x_1 \\ x_N & \ddots & \vdots \\ \boldsymbol{0} & & x_N \end{bmatrix} \quad (6)$$

Rewrite (1) as

$$\boldsymbol{y} = \boldsymbol{X}(\boldsymbol{a}_s \odot \boldsymbol{c}_s) + \boldsymbol{e} \quad (7)$$

Obviously, we transform sampling channel $\boldsymbol{h}$ into sampling $\boldsymbol{a}_s$ and $\boldsymbol{c}_s$.

Now we derive the posteriori distributions for $\boldsymbol{a}_s$ and $\boldsymbol{c}_s$, respectively. In specific, during the nth iteration, starting with $\boldsymbol{x}^{(n-1)} = \{x_0^{(n-1)}, \ldots, x_{N-1}^{(n-1)}\}$, $\boldsymbol{a}_s{}^{(n-1)} = \{a_{s0}^{(n-1)}, \ldots, a_{sL}^{(n-1)}\}$, and $\boldsymbol{c}_s{}^{(n-1)} = \{c_{s0}^{(n-1)}, \ldots, c_{sL}^{(n-1)}\}$, we need to generate $\boldsymbol{a}_s{}^{(n)}$ and $\boldsymbol{c}_s{}^{(n)}$ sequentially. We can get from (3) that $\boldsymbol{h}^{(n-1)} = \boldsymbol{a}_s^{(n-1)} \odot \boldsymbol{c}_s^{(n-1)}$. To derive the posteriori distribution of a_{si}, $i = 0, \ldots L$, from the model in (7) we get

$$\begin{aligned}
&p\left(a_{si}|\boldsymbol{x}, \boldsymbol{y}, c_{si}, \overline{\boldsymbol{h}}\right)\\
&\propto p(\boldsymbol{y}|\boldsymbol{x}, \boldsymbol{h})p(a_{si})\\
&\propto \exp\left(-\frac{1}{\sigma^2}\|\boldsymbol{y}-\boldsymbol{X}\boldsymbol{h}\|_2^2\right)\cdot p(a_{si})\\
&\propto \exp\left\{-\frac{1}{\sigma^2}\left[\|\boldsymbol{X}\boldsymbol{h}\|_2^2 - 2Re\left(\boldsymbol{y}^H\boldsymbol{X}\boldsymbol{h}\right)\right]\right\}\cdot p(a_{si})\\
&\propto \exp\left\{-\frac{1}{\sigma^2}\left[\sum_i h_i\boldsymbol{x}_{i0}^H\sum_j h_j\boldsymbol{x}_{j0} - 2Re\left(\boldsymbol{y}^H\sum_i h_i\boldsymbol{x}_{i0}\right)\right]\right\}\\
&\quad\cdot p(a_{si})\\
&\propto \exp\left\{-\frac{1}{\sigma^2}\left[\boldsymbol{x}_{l0}^H\boldsymbol{x}_{l0}(a_{si}c_{si})^2 + 2Re\left[\left(\sum_{i\neq l}h_i\boldsymbol{x}_{i0}^H\right)\boldsymbol{x}_{l0}\right]\right.\right.\\
&\quad\left.\left. a_{si}c_{si} - 2Re\left(\boldsymbol{y}^H\boldsymbol{x}_{l0}\right)a_{si}c_{si}\right]\right\}\cdot p(a_{si})\\
&\propto \exp\left\{-\frac{N\varepsilon_x}{\sigma^2}(a_{si}c_{si})^2 + \frac{2}{\sigma^2}Re\left[\left(\boldsymbol{y}^H - \sum_{i\neq l}h_i\boldsymbol{x}_{i0}^H\right)\boldsymbol{x}_{l0}\right]\right.\\
&\quad\left. a_{si}c_{si}\right\}\cdot p(a_{si})\\
&= \begin{cases} A\cdot\exp\left\{-\frac{N\varepsilon_x}{\sigma^2}c_{si}^2 + \frac{2}{\sigma^2}Re\left[\left(\boldsymbol{y}^H - \sum_{i\neq l}h_i\boldsymbol{x}_{i0}^H\right)\boldsymbol{x}_{l0}\right]\right.\\ \quad\left. c_{si}\right\}\cdot q,\ a_{si}=1\\ A\cdot(1-q),\ a_{si}=0\end{cases}
\end{aligned}\tag{8}$$

where ε_x is the energy of transmitted symbols, $\Re(\cdot)$ represents the real part of the corresponding term.

Similarly we can get

$$\begin{aligned}
&p(c_{si}|\boldsymbol{x}, \boldsymbol{y}, \overline{\boldsymbol{h}}, a_{si}=1)\\
&\propto p(\boldsymbol{y}|\boldsymbol{x}, \boldsymbol{h})p(c_{si})\\
&\propto \exp(-\frac{1}{\sigma^2}\|\boldsymbol{y}-\boldsymbol{X}\boldsymbol{h}\|_2^2)\cdot\exp(-c_{si}^2/\sigma_0^2)\\
&\propto \exp\left\{-\frac{1}{\sigma^2}\left[\|\boldsymbol{X}\boldsymbol{h}\|_2^2 - 2Re(\boldsymbol{y}^H\boldsymbol{X}\boldsymbol{h})\right] - c_{si}^2/\sigma_0^2\right\}\\
&\propto \exp\left\{-\frac{1}{\sigma^2}\left[\sum_i h_i\boldsymbol{x}_{i0}^H\sum_j h_j\boldsymbol{x}_{j0} - 2Re\left(\boldsymbol{y}^H\sum_i h_i\boldsymbol{x}_{i0}\right)\right]\right.\\
&\quad\left. - c_{si}^2/\sigma_0^2\right\}\\
&\propto \exp\left\{-\frac{1}{\sigma^2}\left[\boldsymbol{x}_{l0}^H\boldsymbol{x}_{l0}c_{si}^2 + 2Re\left[\left(\sum_{i\neq l}h_i\boldsymbol{x}_{i0}^H\right)\boldsymbol{x}_{l0}\right]c_{si}\right.\right.\\
&\quad\left.\left. - 2Re\left(\boldsymbol{y}^H\boldsymbol{x}_{l0}\right)c_{si}\right] - c_{si}^2/\sigma_0^2\right\}\\
&\propto \exp\left\{-\left(\frac{K\varepsilon_x}{\sigma^2}+\frac{1}{\sigma_0^2}\right)c_{si}^2 + \frac{2}{\sigma^2}Re\left[\left(\boldsymbol{y}^H - \sum_{i\neq l}h_i\boldsymbol{x}_{i0}^H\right)\boldsymbol{x}_{l0}\right]\right.\\
&\quad\left.\cdot c_{si}\right\}\\
&\sim N\left(\frac{b_1}{2a}, \frac{1}{a}\right)
\end{aligned}\tag{9}$$

where

$$a = \frac{K\varepsilon_x}{\sigma^2} + \frac{1}{\sigma_0^2}$$

$$b_1 = \frac{2}{\sigma^2}\Re\left[\left(\boldsymbol{y}^H - \sum_{i\neq l}h_i\boldsymbol{x}_{i0}^H\right)\boldsymbol{x}_{l0}\right]\tag{10}$$

One can obtain a noninformative prior by letting $\sigma_0^2 \to \infty$, then a turns into

$$a = \frac{K\varepsilon_x}{\sigma^2}\tag{11}$$

We also have

$$p(c_{si}|\boldsymbol{x}, \boldsymbol{y}, \overline{\boldsymbol{h}}, a_{si}=0) = \delta(c_{si})\tag{12}$$

2) SAMPLING SPARSE CHANNELS IN OFDM SYSTEMS

Rewrite (2) as

$$\boldsymbol{y}_F = diag\{\boldsymbol{x}\}\boldsymbol{F}\left(\boldsymbol{a}_{s0}\cdot\boldsymbol{c}_{s0}\right) + \boldsymbol{w}_F\tag{13}$$

To derive the posterior distribution of a_{si} for OFDM systems, from the model in (13) we get

$$\begin{aligned}
&p(a_{si}|\boldsymbol{x}, \boldsymbol{y}_F, c_{si}, \bar{\boldsymbol{h}})\\
&\propto p(\boldsymbol{y}_F|\boldsymbol{x}, \boldsymbol{h})p(a_{si})\\
&\propto \exp\left(-\frac{1}{\sigma^2}\left\|\boldsymbol{y}_F - diag\{\boldsymbol{x}\}\boldsymbol{F}\boldsymbol{h}\right\|_2^2\right)\cdot p(a_{si})\\
&= \begin{cases} B\cdot\exp\left[-\frac{K\varepsilon_x}{\sigma^2}c_{si}^2 + \frac{2}{\sigma^2}\Re\left(\sum_{k=1}^{K}y_{Fk}^*x_kF_{kl}\right)c_{si}\right]\\ \cdot q,\ a_{si}=1\\ B\cdot(1-q),\ a_{si}=0\end{cases}
\end{aligned}\tag{14}$$

where y_{Fk}^* denotes the kth element of $\boldsymbol{y}_F$, F_{kl} denotes the (k, l) element of the DFT matrix $\boldsymbol{F}$.

Similarly we can get

$$\begin{aligned}
&p(c_{si}|\boldsymbol{x}, \boldsymbol{y}_F, \bar{\boldsymbol{h}}, a_{si}=1)\\
&\propto p(\boldsymbol{y}_F|\boldsymbol{x}, \boldsymbol{h})p(c_{si})\\
&\propto \exp\left(-\frac{1}{\sigma^2}\left\|\boldsymbol{y}_F - diag\{\boldsymbol{x}\}\boldsymbol{F}\boldsymbol{h}\right\|_2^2\right)\cdot\exp(-c_{si}^2/\sigma_0^2)\\
&\propto \exp\left[-\left(\frac{K\varepsilon_x}{\sigma^2}+\frac{1}{\sigma_0^2}\right)c_{si}^2 + \frac{2}{\sigma^2}\Re\left(\sum_{k=1}^{K}y_{Fk}^*x_kF_{kl}\right)c_{si}\right]\\
&\sim N\left(\frac{b_2}{2a}, \frac{1}{a}\right)
\end{aligned}\tag{15}$$

where

$$b_2 = \frac{2}{\sigma^2}\Re\left(\sum_{k=1}^{K}y_{Fk}^*x_kF_{kl}\right)\tag{16}$$

and K denotes the number of subcarriers in OFDM systems. We also get

$$p(c_{si}|\boldsymbol{x}, \boldsymbol{y}_F, \bar{\boldsymbol{h}}, a_{si}=0) = \delta(c_{si})\tag{17}$$

C. GIBBS SAMPLING OF TRANSMITTED SYMBOLS

During the nth iteration, starting with $\boldsymbol{x}^{(n-1)} = \{x_0^{(n-1)}, \ldots, x_{N-1}^{(n-1)}\}$ $\boldsymbol{a}_s{}^{(n)}$ and $\boldsymbol{c}_s{}^{(n)}$, $\boldsymbol{x}^{(n)}$ is generated bit by bit sequentially (for SC systems) or parallelly (for OFDM systems).

1) SAMPLING TRANSMITTED SYMBOLS FOR SC SYSTEMS

In [27], the authors have derived the sampling procedure to obtain samples for binary symbols. It is straightforward to extend the procedure to our finite alphabet set $\mathcal{A}$. In specific, assuming that x_0 through x_{k-1} have been updated during the nth iteration, given by $x_0^{(n)}, \ldots, x_{k-1}^{(n)}$, and symbols $x_{k+1}^{(n-1)}, \ldots, x_{N-1}^{(n-1)}$ are updated during the $(n-1)$th iteration, now we need to update $x_k^{(n)}$.

The sample $x_k^{(n)}$ is generated on the conditional probability distribution $\{\gamma_g, g = Q_1, Q_2, \ldots, Q_{|A|}\}$, where

$$\gamma_g = P(x_k = g|\bar{\boldsymbol{x}}_k, \boldsymbol{y}) \tag{18}$$

and

$$\bar{\boldsymbol{x}}_k = \{x_0^{(n)}, \ldots, x_{k-1}^{(n)}, x_{k+1}^{(n-1)}, \ldots, x_{T-1}^{(n-1)}\} \tag{19}$$

From (3) we get $\boldsymbol{h}^{(n)} = \boldsymbol{a}_s{}^{(n)} \odot \boldsymbol{c}_s{}^{(n)}$. Define $\boldsymbol{x}^g = \{x_0^{(n)}, \ldots, x_{k-1}^{(n)}, g, x_{k+1}^{(n-1)}, \ldots, x_{T-1}^{(n-1)}\}$ for each $g = \{Q_1, Q_2, \ldots, Q_{|A|}\}$. By assuming a uniform prior distribution for $P(x_k = g)$, we get

$$\begin{aligned}\gamma_g &= p(x_k = g|\bar{\boldsymbol{x}}_k, \boldsymbol{y}) \propto p(\boldsymbol{y}|\boldsymbol{x}^g)P(x_k = g)\\ &\propto p(\boldsymbol{y}|\boldsymbol{x}^g) = \prod_{j=0}^{N+L-1} p(y_j|\boldsymbol{x}^g_{j-L:j})\\ &= \left\{\prod_{j=0}^{k-1} p(y_j|\boldsymbol{x}^g_{j-L:j}) \prod_{j=k+L+1}^{N+L-1} p(y_j|\boldsymbol{x}^g_{j-L:j})\right\}\\ &\quad\times \prod_{j=k}^{k+L} p(y_j|\boldsymbol{x}^g_{j-L:j}))\end{aligned} \tag{20}$$

where $\boldsymbol{x}_{j-L:j} = [x_{j-L}, x_{j-L+1}, \ldots, x_j]^T$. When $j \le k-1$ or $j \ge k+L+1$, the vector $\boldsymbol{x}^g_{j-L:j}$ is independent of g. Thus,(20) is simplified to

$$\begin{aligned}\gamma_g &\propto \prod_{j=k}^{k+L} p(y_j|\boldsymbol{x}^g_{j-L:j})\\ &= C \cdot \exp\left\{\sum_{j=k}^{k+L}\left(-\frac{1}{2\sigma^2}\left|y_j - \sum_{l=0}^{L} h_l x^g_{j-l}\right|^2\right)\right\}\end{aligned} \tag{21}$$

where C is a scaling constant to ensure that $\sum_g \gamma_g = 1$.

2) SAMPLING TRANSMITTED SYMBOLS FOR OFDM SYSTEMS

From (3) we have $\boldsymbol{h}^{(n)} = \boldsymbol{a}_s{}^{(n)} \odot \boldsymbol{c}_s{}^{(n)}$. For each $g = \{Q_1, Q_2, \ldots, Q_{|A|}\}$, from (2) we get

$$\begin{aligned}\gamma_g &= P(x_k = g|y_{Fk}) \propto P(y_{Fk}|x_k = g)P(x_k = g)\\ &\propto p(y_{Fk}|x_k = g) = C \cdot \exp\left[-\frac{1}{\sigma^2}|y_{Fk} - g h_{Fk}|^2\right]\end{aligned} \tag{22}$$

where C is a scaling constant, h_{Fk} is the kth element of $\boldsymbol{h}_F$, $\boldsymbol{h}_F$ is defined as $\boldsymbol{h}_F \triangleq \boldsymbol{F}\boldsymbol{h}$, and we assume a uniform prior distribution for $P(x_k = g)$.

Our proposed algorithm is summarized in Algorithm 1 below.

Algorithm 1 Proposed Algorithm

1. Set iteration counter to $j = 1$, and set the initialize value of the unknown parameters randomly.
2. Sample from (8)-(9) for SC systems or (14)-(15) for OFDM systems to obtain samples of sparsity pattern and sparse coefficient.
3. Sample from (21) for SC systems or (22) for OFDM systems.
4. Change iteration counter from j to $j+1$ and return to step 2 until convergence or maximum iteration.

After specifying the length of the "burn-in" period J, it is reasonable to approximate $\boldsymbol{h}^{(n)} = \boldsymbol{a}_s^{(n)} \odot \boldsymbol{c}_s^{(n)} \sim p(\boldsymbol{h}|\boldsymbol{y})$, $\boldsymbol{x}^{(n)} \sim p(\boldsymbol{x}|\boldsymbol{y})$ for $n = J+1, \ldots, I$. The transmitted symbols are first estimated as $\hat{\boldsymbol{x}} = (1/(I-J)) \sum_{n=J+1}^{I} \boldsymbol{x}^{(n)}$. Then the final hard decision is made by slicing every element in $\hat{\boldsymbol{x}}$ to its nearest constellation point.

Note that the dominant computational complexity of our proposed algorithm comes from sampling of transmitted symbols. Therefore, we focus on computation of (21), and it turns out that the computational complexity of (21) is $O(Nh_e^2|\mathcal{A}|)$ per iteration, where h_e denotes the effective number of path in sparse channels. Hence the total complexity is of $O(Nh_e^2|\mathcal{A}|I)$.

D. EXTENSION TO TIME-VARYING UNDERWATER ACOUSTIC CHANNELS

Previously we have assumed that the channel remains constant over observed samples. Now we extend our proposed algorithm to time-varying underwater acoustic channels. The block diagram of the proposed receiver is shown in Fig. 1. The components of sparse channel sampling, transmitted symbols sampling and symbol detection have been discussed by assuming static channels in previous subsections. Now we elaborate extra components which handle time-varying characteristics of underwater acoustic channels.

1) TIME-VARYING UNDERWATER ACOUSTIC CHANNEL MODELING

A popular method to model time-varying characteristics of underwater acoustic channels is by modeling linear path delays with respect to Doppler scaling factors while keeping path gains as constants as in [9], [10], [34]. Following this approach, the impulse responses of time-varying underwater acoustic channels could be modeled as

$$h(t;\tau) = \sum_l A_l \delta(\tau - (\tau_l - at)) \tag{23}$$

where τ_l, A_l and a denote the path delay, path gain and Doppler scaling factor, respectively. At the receiver, by resampling the received signal in passband [35], [36], one can obtain

$$\tilde{y}(t) = Re\left\{\sum_l A_l x_b\left(\frac{1+a}{1+b}t - \tau_l\right) e^{j2\pi f_c\left(\frac{1+a}{1+b}t - \tau_l\right)}\right\} + \tilde{n}(t) \tag{24}$$

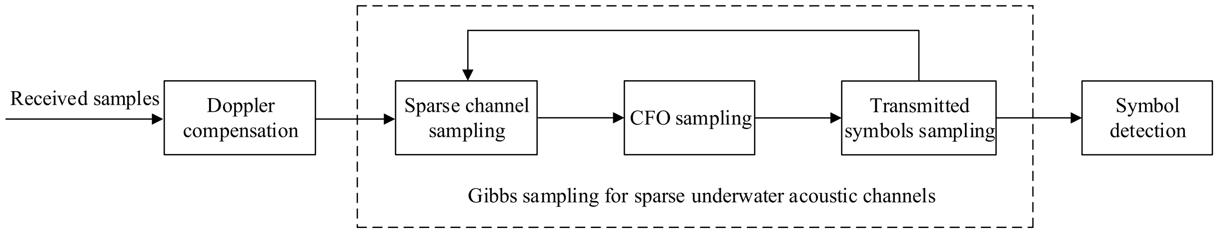

FIGURE 1. **The block diagram of the proposed receiver.**

where b denotes the resampling factor, $x_b(t)$ represents the baseband equivalent transmitted signal, f_c is the carrier frequency, and $\tilde{n}(t)$ is the additive noise.

2) DOPPLER COMPENSATION

Coarse Doppler scaling factor estimation can be computed by simply comparing the time duration of transmitted packet and received packet as in [34], [35]. Then the baseband equivalent received signal after Doppler compensation via resampling can be similarly approximated as in [34] by

$$y(t) = e^{j2\pi\varepsilon t}\sum_l A_l x_b\left(t-\tau_l\right)e^{-j2\pi f_c\tau_l} + n(t) \tag{25}$$

The discrete version of received samples can be obtained by

$$y_n = e^{j2\pi\varepsilon nT}\sum_{l=0}^{L} h_l x_{n-l} + w_n, \quad n = 0, 1, \ldots, N-1+L \tag{26}$$

where $\varepsilon = \frac{a-b}{1+b}f_c$ denotes a Doppler shift and is called carrier frequency offset (CFO) since its role is similar as CFO in radio communications [15], [34].

3) CFO SAMPLING

Rewrite (26) in matrix form as

$$\boldsymbol{y} = \boldsymbol{Q}\boldsymbol{X}\left(\boldsymbol{a}_s \odot \boldsymbol{c}_s\right) + \boldsymbol{e} \tag{27}$$

where

$$\boldsymbol{Q} = diag\left\{1, e^{j2\pi\varepsilon_1/(N+L-1)}, e^{j4\pi\varepsilon_1/(N+L-1)}, \cdots e^{j2\pi\varepsilon_1}\right\}$$

$\varepsilon_1 = \varepsilon T(N+L-1)$ denotes the normalized CFO, and T is symbol interval.

Note that the model in (27) is nonlinear with respect to the normalized CFO ε_1. Correspondingly, the posteriori distribution of ε_1 is not standard, leading to the difficulties of sampling from the posteriori distribution. To circumvent this problem, in [26] and our previous work [37], the second order truncated Taylor series approximation with respect to the CFO term is adopted to facilitate Gibbs sampling. One can use similar method to derive the posteriori distribution for ε_1.

In particular, we choose a conjugate normal prior distribution for ε_1 as

$$p(\varepsilon_1) = \frac{1}{\sqrt{2\pi\sigma^2_{\varepsilon_{1p}}}}\exp\left\{-\frac{(\varepsilon_1-\mu_{\varepsilon_{1p}})^2}{2\sigma^2_{\varepsilon_{1p}}}\right\} \tag{28}$$

with $\mu_{\varepsilon_{1p}}$ and $\sigma^2_{\varepsilon_{1p}}$ being associated hyper parameters. One can approximate the exponential term $\exp\{j2\pi n\varepsilon_1/(N+L-1)\}$ (with $n = 0, 1, \ldots, N+L-1$) in $\boldsymbol{Q}$ with its second order truncated Taylor series expansion

$$\begin{aligned}&\exp\left\{\frac{j2\pi n\varepsilon_1}{N+L-1}\right\}\\ &\simeq \exp\left\{\frac{j2\pi n\tilde{\varepsilon}_1}{N+L-1}\right\}\\ &\quad+\frac{j2\pi n}{N+L-1}\exp\left\{\frac{j2\pi n\tilde{\varepsilon}_1}{N+L-1}\right\}(\varepsilon_1-\tilde{\varepsilon}_1)\\ &\quad-\frac{2\pi^2n^2}{(N+L-1)^2}\exp\left\{\frac{j2\pi n\tilde{\varepsilon}_1}{N+L-1}\right\}(\varepsilon_1-\tilde{\varepsilon}_1)^2\end{aligned} \tag{29}$$

developed around the last available sample of $\tilde{\varepsilon}_1$ (drawn at the previous iteration). By defining

$$\begin{cases}\boldsymbol{Q}_{10} = diag\left\{\exp\left(\frac{j2\pi n\cdot\tilde{\varepsilon}_1}{N+L-1}\right)\right\}\\ \boldsymbol{Q}_{11} = diag\left\{\frac{j2\pi n}{N+L-1}\cdot\exp\left(\frac{j2\pi n\cdot\tilde{\varepsilon}_1}{N+L-1}\right)\right\}\\ \boldsymbol{Q}_{12} = diag\left\{-\frac{2\pi^2n^2}{(N+L-1)^2}\exp\left(\frac{j2\pi n\tilde{\varepsilon}_1}{N+L-1}\right)\right\}\end{cases}$$

$\boldsymbol{Q}$ is approximated by

$$\boldsymbol{Q} \simeq \boldsymbol{Q}_{10} + \boldsymbol{Q}_{11}(\varepsilon_1-\tilde{\varepsilon}_1) + \boldsymbol{Q}_{12}(\varepsilon_1-\tilde{\varepsilon}_1)^2 \tag{30}$$

It is straightforward to derive the posteriori distribution of ε_1 as

$$\begin{aligned}&p(\varepsilon_1|\boldsymbol{x},\boldsymbol{y},\boldsymbol{a}_s,\boldsymbol{c}_s)\\ &\propto p(\boldsymbol{y}|\boldsymbol{x},\boldsymbol{a}_s,\boldsymbol{c}_s,\varepsilon_1)\cdot p(\varepsilon_1)\\ &\propto \exp\left(-\frac{1}{\sigma^2}\left\|\boldsymbol{y}-\boldsymbol{Q}\boldsymbol{X}\left(\boldsymbol{a}_s\odot\boldsymbol{c}_s\right)\right\|_2^2\right)\cdot p(\varepsilon_1)\\ &\propto \exp\left\{\frac{2Re\left(\boldsymbol{y}^H\boldsymbol{Q}(\boldsymbol{a}_s\odot\boldsymbol{c}_s)^H\boldsymbol{X}^H\right)}{\sigma^2}-\frac{(\varepsilon_1-\mu_{\varepsilon_{1p}})^2}{2\sigma^2_{\varepsilon_{1p}}}\right\}\\ &\sim(\mu_{\varepsilon_1},\sigma^2_{\varepsilon_1})\end{aligned} \tag{31}$$

where

$$\sigma^2_{\varepsilon_1} = \left\{\frac{1}{\sigma^2_{\varepsilon_{1p}}}-\frac{4}{\sigma^2}Re\left[\boldsymbol{t}_\varepsilon\boldsymbol{Q}_{12}^H\boldsymbol{y}\right]\right\}^{-1} \tag{32}$$

$$\begin{aligned}\mu_{\varepsilon_1} &= \frac{-4\sigma^2_{\varepsilon_1}}{\sigma^2}\left[-Re\left(\boldsymbol{t}_\varepsilon\boldsymbol{Q}_{11}^H\boldsymbol{y}\right)/2+\tilde{\varepsilon}_1 Re\left(\boldsymbol{t}_\varepsilon\boldsymbol{Q}_{12}^H\boldsymbol{y}\right)\right]\\ &\quad-\mu_{\varepsilon_{1p}}/(2\sigma^2_{\varepsilon_{1p}})\end{aligned} \tag{33}$$

and $\boldsymbol{t}_\varepsilon = (\boldsymbol{a}_s\odot\boldsymbol{c}_s)^H\boldsymbol{X}^H$.

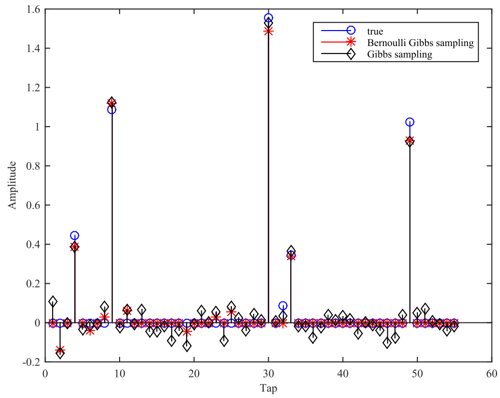

FIGURE 2. Samples drawn by the proposed sparse sampling algorithm and normal Gibbs sampling algorithm when $E_b/N_0 = 5dB$.

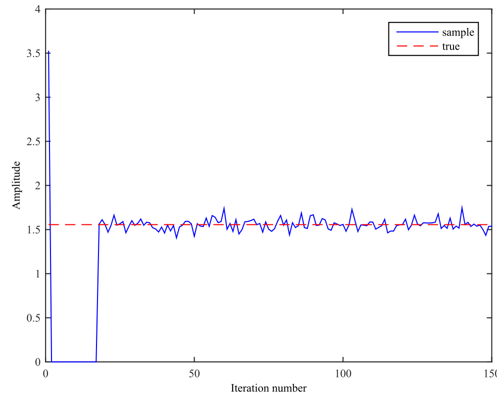

FIGURE 3. Samples drawn by the proposed algorithm for the most significant tap of the channel in Fig 2 when $E_b/N_0 = 5dB$.

One can obtain a noninformative prior by letting $\sigma^2_{\varepsilon_{1p}} \to \infty$, then (32) and (33) turn into

$$\sigma^2_{\varepsilon_1} = -\frac{\sigma^2}{4}\left\{Re\left[\boldsymbol{t}_\varepsilon \boldsymbol{Q}_{12}^H \boldsymbol{y}\right]\right\}^{-1} \tag{34}$$

$$\mu_{\varepsilon_1} = \frac{-4\sigma^2_{\varepsilon_1}}{\sigma^2}\left[-Re\left(\boldsymbol{t}_\varepsilon \boldsymbol{Q}_{11}^H \boldsymbol{y}\right)/2 + \tilde{\varepsilon}_1 Re\left(\boldsymbol{t}_\varepsilon \boldsymbol{Q}_{12}^H \boldsymbol{y}\right)\right] \tag{35}$$

Clearly, our algorithm could be extended to time-varying underwater acoustic channels by simply adding an extra sampling step from (31).

IV. SIMULATION RESULTS

The BPSK modulation is used with the block length $N = 256$. Firstly, by using pilot symbols of the whole transmitting block, Fig. 2 compares channel samples from our proposed algorithm with traditional Gibbs sampling algorithm when $E_b/N_0 = 5dB$. Obviously, the channel samples from our proposed algorithm are more sparse and accurate compared with traditional Gibbs sampling algorithm.

To assess the convergence of the proposed algorithm, the output of the Markov chains have been monitored. In Fig. 2, the first 150 samples of the most significant tap of the channel in Fig. 2 are shown. These results provide strong evidence that the proposed algorithm quickly converges to the true parameters. Note that initial samples are zeros because the samples for sparsity pattern did not converge. For other channel taps and transmitted symbols, we observe similar behaviors. Furthermore, we also calculate the mean squared errors of estimated parameters and evaluate the reconstruction error as a function of the iteration number as in [1]. Based on these tests, which are not shown here for brevity, the burn-in and run lengths for proposed algorithm are set to 40 and 150, respectively, which provides some safety margin.

Next we fix the channel delay spread as $L = 55$. The entries of sparsity pattern are drawn i.i.d. from Bernoulli distribution with parameter $q = 0.1$ as described in Section II. The sparse coefficient is drawn i.i.d from standard normal distribution. Assuming the transmitted symbols are known at the receiver, the MSE performance of channel estimation by the proposed algorithm with traditional Gibbs sampling algorithm is shown in Fig. 4. Clearly, our proposed algorithm outperforms the traditional Gibbs sampling algorithm by incorporating channel sparsity. The more accurate channel information naturally leads to more improved BER performance.

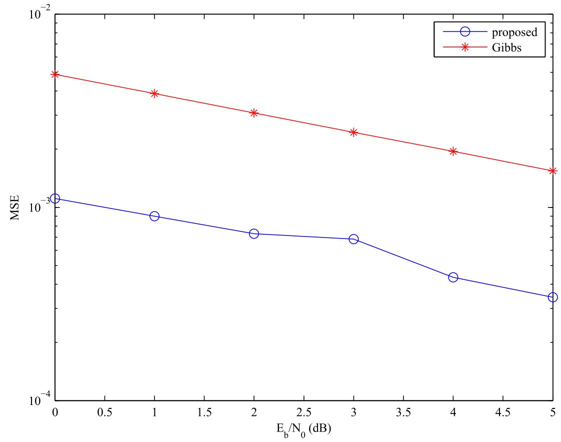

FIGURE 4. The MSE performance of channel estimation.

Then we focus on BER performance. The superimposed modulus of the true channel response $\boldsymbol{h}$ and the channel response initialization $\boldsymbol{h}^{(0)}$ are shown in Fig. 5. The mismatch between $\boldsymbol{h}$ and $\boldsymbol{h}^{(0)}$ ($\left\|\boldsymbol{h} - \boldsymbol{h}^{(0)}\right\|_2 = 2.40$) is for the purpose of evaluating an outdated channel response initialization.

Fig. 6 shows the BER performance of proposed algorithm and traditional Gibbs sampling algorithm. We can see that our algorithm significantly outperforms traditional Gibbs sampling algorithm, especially for high SNR region. The reason is that our proposed algorithm could generate more sparse and accurate channel samples, as demonstrated in Fig. 2 and Fig. 4. The gap between two algorithms gets larger with increased SNR.

Fig. 7 tests the effects of the parameter q of Bernoulli distribution. From Fig. 5 we can observe that there are 6 nonzero taps out of delay spread $L = 55$. Therefore the correct q should be $q = 6/55 = 0.1$. When $q = 0.2$ is

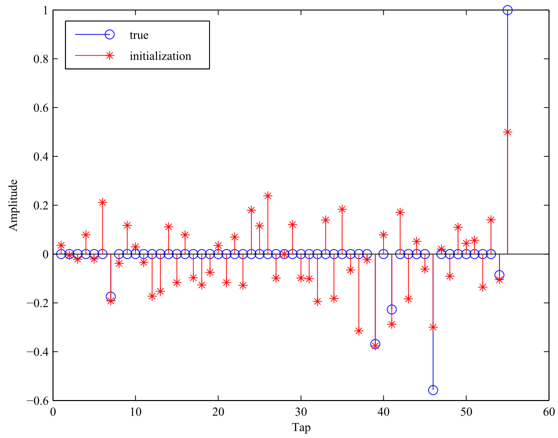

FIGURE 5. The modulus of the true channel response and channel response initialization.

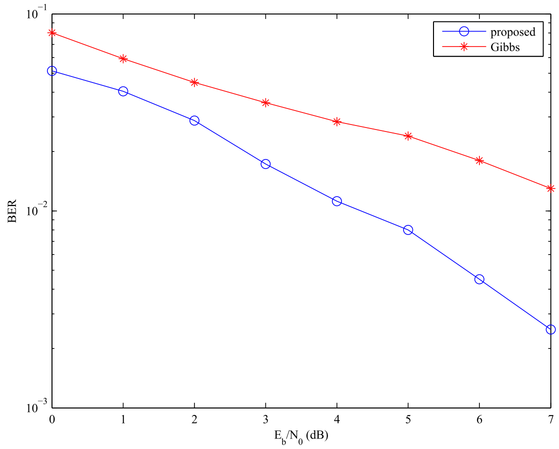

FIGURE 6. Performance comparisons of various receivers over the sparse channel.

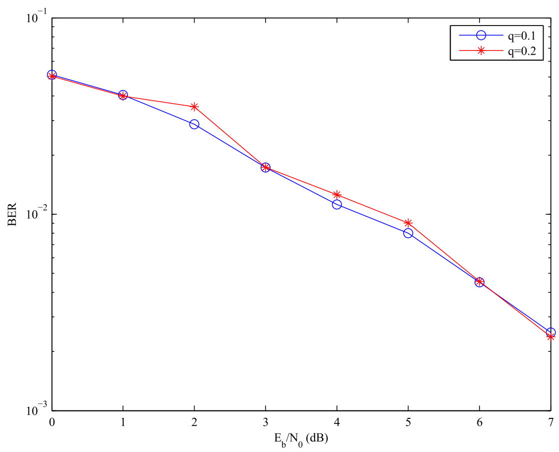

FIGURE 7. The effect of different q when $E_b/N_0 = 5dB$.

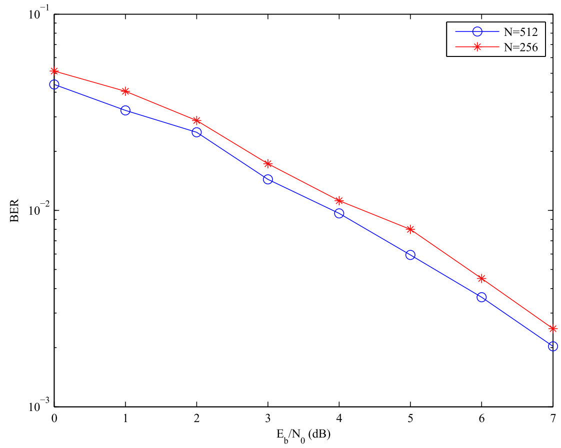

FIGURE 8. Performance comparisons with different frame size over the sparse channel.

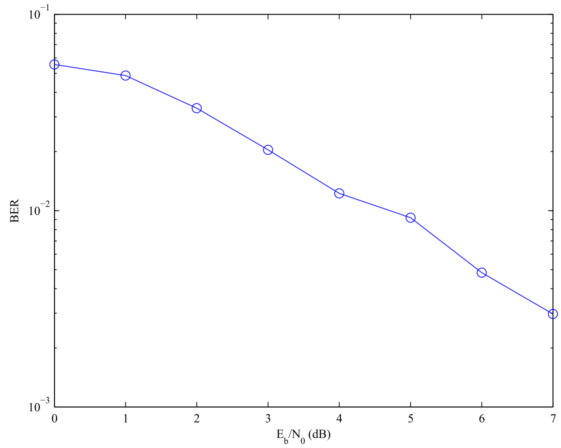

FIGURE 9. BER performance for the OFDM system.

used, the resulting BER performance is similar as shown in Fig. 7. We can observe that our proposed algorithm is robust to selecting q.

We then exhibit the BER performance with respect to block length. The BER results with block lengths of $N = 512$ and $N = 256$ are shown in Fig. 8, respectively. Intuitively, BER performance should be improved with the increase of the block length since the unknown channel is assumed to be static during a whole block. Indeed, one can observe from Fig. 8 that the BER performance gets improved by increasing the block length. On the other hand, the assumption of static channel for whole transmitting block gets weaker with increase of block length.

In Fig. 9 we show the BER performance of proposed algorithm for the OFDM system. 256 subcarriers each with BPSK modulation are used in the OFDM system. One can observe comparable BER performance with SC counterpart shown in Fig. 6.

Finally, we test our proposed algorithm in the time-varying underwater acoustic channel. Based on the experimental results from [34], we choose the CFO $\varepsilon = 5Hz$ in the simulation. We further assume $T = 2 \times 10^{-4}s$, corresponding to the transmission rate of $5kbps$. The normalized CFO with $N = 256$ is then $\varepsilon_1 = 0.31$. Fig. 10 shows the BER results in the time-varying underwater acoustic channel. The resulting BER performance is similar as the results in the

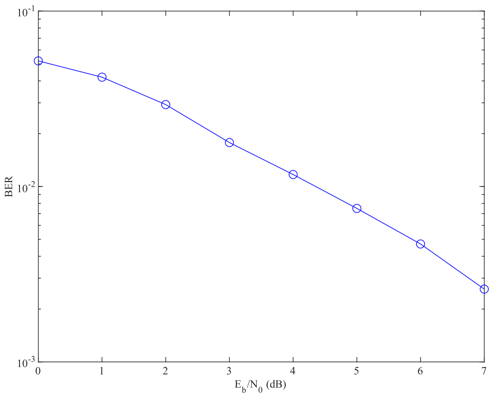

FIGURE 10. BER performance in the time-varying underwater acoustic channel.

static channel as shown in Fig. 6, demonstrating our proposed algorithm could work well in time-varying underwater acoustic channels.

V. CONCLUSION AND FUTURE WORK

This paper investigates semiblind equalizer for sparse underwater acoustic channels. Existing related works assumed non-sparse channels, and could not work well in sparse channels. In this manuscript, we have proposed a Gibbs-based semi-blind equalization algorithm for sparse channels. Different from existing literature using conjugate priors for channels, we decompose the sparse channel response into components of sparsity pattern and sparse coefficient, and incorporate the sparse structures of channels in Bernoulli prior probability distributions for sparsity pattern. We derive the posterior distributions for both sparsity pattern and sparse coefficient components, thereby sampling of sparse channels could be obtained. Traditional Gibbs sampling algorithm could be viewed as a special case of our proposed algorithm. Moreover, our algorithm could be applied in underwater acoustic channels. Numerical results are provided to demonstrate performance of proposed algorithm. Future work in this field includes the application of the proposed algorithm with data from sea or lake experiments.

REFERENCES

[1] M. Chitre, S. Shahabudeen, and M. Stojanovic, "Underwater acoustic communications and networking: Recent advances and future challenges," *Mar. Technol. Soc. J.*, vol. 42, no. 1, pp. 103–116, Mar. 2008.

[2] D. B. Kilfoyle and A. B. Baggeroer, "The state of the art in underwater acoustic telemetry," *IEEE J. Ocean. Eng.*, vol. 25, no. 1, pp. 4–27, Jan. 2000.

[3] J. C. Preisig and G. B. Deane, "Surface wave focusing and acoustic communications in the surf zone," *J. Acoust. Soc. Amer.*, vol. 116, no. 4, pp. 2067–2080, Oct. 2004.

[4] J. A. Catipovic, "Performance limitations in underwater acoustic telemetry," *IEEE J. Ocean. Eng.*, vol. 15, no. 3, pp. 205–216, Jul. 1990.

[5] J. Preisig, "Acoustic propagation considerations for underwater acoustic communications network development," *ACM SIGMOBILE Mobile Comput. Commun. Rev.*, vol. 11, no. 4, pp. 2–10, Oct. 2007.

[6] W. Li and J. C. Preisig, "Estimation of rapidly time-varying sparse channels," *IEEE J. Ocean. Eng.*, vol. 32, no. 4, pp. 927–939, Oct. 2007.

[7] S. Roy, T. M. Duman, and V. K. McDonald, "Error rate improvement in underwater MIMO communications using sparse partial response equalization," *IEEE J. Ocean. Eng.*, vol. 34, no. 2, pp. 181–201, Apr. 2009.

[8] J. W. Choi, T. J. Riedl, K. Kim, A. C. Singer, and J. C. Preisig, "Adaptive linear turbo equalization over doubly selective channels," *IEEE J. Ocean. Eng.*, vol. 36, no. 4, pp. 473–489, Oct. 2011.

[9] Z. Wang, S. Zhou, G. B. Giannakis, C. R. Berger, and J. Huang, "Frequency-domain oversampling for zero-padded OFDM in underwater acoustic communications," *IEEE J. Ocean. Eng.*, vol. 37, no. 1, pp. 14–24, Jan. 2012.

[10] Z. Wang, S. Zhou, J. Catipovic, and J. Huang, "Factor-graph-based joint IBI/ICI mitigation for OFDM in underwater acoustic multipath channels with long-separated clusters," *IEEE J. Ocean. Eng.*, vol. 37, no. 4, pp. 680–694, Oct. 2012.

[11] K. Pelekanakis and M. Chitre, "New sparse adaptive algorithms based on the natural gradient and the L_0-norm," *IEEE J. Ocean. Eng.*, vol. 38, no. 2, pp. 323–332, Apr. 2013.

[12] K. Tu, T. M. Duman, M. Stojanovic, and J. G. Proakis, "Multiple-resampling receiver design for OFDM over Doppler-distorted underwater acoustic channels," *IEEE J. Ocean. Eng.*, vol. 38, no. 2, pp. 333–346, Apr. 2013.

[13] A. Radosevic, R. Ahmed, T. M. Duman, J. G. Proakis, and M. Stojanovic, "Adaptive OFDM modulation for underwater acoustic communications: Design considerations and experimental results," *IEEE J. Ocean. Eng.*, vol. 39, no. 2, pp. 357–370, Apr. 2014.

[14] S.-H. Byun, W. Seong, and S.-M. Kim, "Sparse underwater acoustic channel parameter estimation using a wideband receiver array," *IEEE J. Ocean. Eng.*, vol. 38, no. 4, pp. 718–729, Oct. 2013.

[15] F. Qu, X. Nie, and W. Xu, "A two-stage approach for the estimation of doubly spread acoustic channels," *IEEE J. Ocean. Eng.*, vol. 40, no. 1, pp. 131–143, Jan. 2015.

[16] Z. Yang and Y. Rosa Zheng, "Iterative channel estimation and turbo equalization for multiple-input multiple-output underwater acoustic communications," *IEEE J. Ocean. Eng.*, vol. 41, no. 1, pp. 232–242, Jan. 2016.

[17] K. Pelekanakis and M. Chitre, "Robust equalization of mobile underwater acoustic channels," *IEEE J. Ocean. Eng.*, vol. 40, no. 4, pp. 775–784, Oct. 2015.

[18] W. Li, S. Zhou, P. Willett, and Q. Zhang, "Preamble detection for underwater acoustic communications based on sparse channel identification," *IEEE J. Ocean. Eng.*, vol. 44, no. 1, pp. 256–268, Jan. 2019.

[19] Y. Zhang, R. Venkatesan, O. A. Dobre, and C. Li, "Efficient estimation and prediction for sparse time-varying underwater acoustic channels," *IEEE J. Ocean. Eng.*, vol. 45, no. 3, pp. 1112–1125, Jul. 2020.

[20] Y. Zakharov, B. Henson, R. Diamant, Y. Fei, P. D. Mitchell, N. Morozs, L. Shen, and T. C. Tozer, "Data packet structure and modem design for dynamic underwater acoustic channels," *IEEE J. Ocean. Eng.*, vol. 44, no. 4, pp. 837–849, Oct. 2019.

[21] Z. Ding and Y. Li, *Blind Equalization and Identification*. New York, NY, USA: Marcel Dekker, 2001.

[22] B. Lu and X. Wang, "Bayesian blind turbo receiver for coded OFDM systems with frequency offset and frequency-selective fading," *IEEE J. Sel. Areas Commun.*, vol. 19, no. 12, pp. 2516–2527, Dec. 2001.

[23] X. Wang and R. Chen, "Blind turbo equalization in Gaussian and impulsive noise," *IEEE Trans. Veh. Technol.*, vol. 50, no. 4, pp. 1092–1105, Jul. 2001.

[24] Z. Yang, B. Lu, and X. Wang, "Bayesian Monte Carlo multiuser receiver for space-time coded multicarrier CDMA systems," *IEEE J. Sel. Areas Commun.*, vol. 19, no. 8, pp. 1625–1637, Aug. 2001.

[25] Z. Yang and X. Wang, "Turbo equalization for GMSK signaling over multipath channels based on the Gibbs sampler," *IEEE J. Sel. Areas Commun.*, vol. 19, no. 9, pp. 1753–1763, Sep. 2001.

[26] F. Z. Merli, X. Wang, and G. M. Vitetta, "A Bayesian multiuser detection algorithm for MIMO-ODFM systems affected by multipath fading, carrier frequency offset, and phase noise," *IEEE J. Sel. Areas Commun.*, vol. 26, no. 3, pp. 506–516, Apr. 2008.

[27] R.-H. Peng, R.-R. Chen, and B. Farhang-Boroujeny, "Markov chain Monte Carlo detectors for channels with intersymbol interference," *IEEE Trans. Signal Process.*, vol. 58, no. 4, pp. 2206–2217, Apr. 2010.

[28] F. Lucka, "Fast Markov chain Monte Carlo sampling for sparse Bayesian inference in high-dimensional inverse problems using L1-type priors," *Inverse Problems*, vol. 28, no. 12, Dec. 2012, Art. no. 125012. [Online]. Available: http://adsabs.harvard.edu/abs/2012InvPr.28l5012L

[29] O. Rabaste and T. Chonavel, "Estimation of multipath channels with long impulse response at low SNR via an MCMC method," *IEEE Trans. Signal Process.*, vol. 55, no. 4, pp. 1312–1325, Apr. 2007.

[30] R.-R. Chen and R. Peng, "Noncoherent detection based on Markov chain Monte Carlo methods for block fading channels," in *Proc. IEEE Global Telecommun. Conf. (GLOBECOM)*, vol. 5, Nov. 2005, p. 2521.

[31] J. Ling and J. Li, "Gibbs-Sampler-Based semiblind equalizer in underwater acoustic communications," *IEEE J. Ocean. Eng.*, vol. 37, no. 1, pp. 1–13, Jan. 2012.
[32] J. Ling, X. Tan, T. Yardibi, J. Li, M. L. Nordenvaad, H. He, and K. Zhao, "On Bayesian channel estimation and FFT-based symbol detection in MIMO underwater acoustic communications," *IEEE J. Ocean. Eng.*, vol. 39, no. 1, pp. 59–73, Jan. 2014.
[33] N. Michelusi, U. Mitra, A. F. Molisch, and M. Zorzi, "UWB sparse/diffuse channels, part I: Channel models and Bayesian estimators," *IEEE Trans. Signal Process.*, vol. 60, no. 10, pp. 5307–5319, Oct. 2012.
[34] B. Li, S. Zhou, M. Stojanovic, L. Freitag, and P. Willett, "Multicarrier communication over underwater acoustic channels with nonuniform Doppler shifts," *IEEE J. Ocean. Eng.*, vol. 33, no. 2, pp. 198–209, Apr. 2008.
[35] B. S. Sharif, J. Neasham, O. R. Hinton, and A. E. Adams, "A computationally efficient Doppler compensation system for underwater acoustic communications," *IEEE J. Ocean. Eng.*, vol. 25, no. 1, pp. 52–61, Jan. 2000.
[36] P.-P.-J. Beaujean and L. R. LeBlanc, "Adaptive array processing for high-speed acoustic communication in shallow water," *IEEE J. Ocean. Eng.*, vol. 29, no. 3, pp. 807–823, Jul. 2004.
[37] Z. Jiang, X. Shen, Y. Ge, R. Zhao, and H. Wang, "Joint time-frequency synchronization and channel estimation in two-way relay networks," *J. Franklin Inst.*, vol. 351, no. 11, pp. 5034–5054, Nov. 2014.

LING WANG received the B.S. degree in computer science from the Academy of Equipment Command and Technology, Beijing, China, in 2002, and the M.S. degree from the School of Astronautics, Northwestern Polytechnical University (NWPU), Xi'an, China, in 2014, where he is currently pursuing the Ph.D. degree with the School of Marine Science and Technology. His research interests include underwater acoustic communications, including channel estimation and equalization, and multicarrier communications.

ZHE JIANG received the B.S. degree in electrical engineering and information science from Xidian University, Xi'an, China, in 2006, and the M.S. and Ph.D. degrees from the School of Marine Science and Technology, Northwestern Polytechnical University (NWPU), Xi'an, in 2008 and 2012, respectively. He joined the School of Marine Science and Technology, NWPU, in 2013, and is currently an Associate Professor. His research interests include communications and signal processing, including channel estimation and equalization, multicarrier communications, space-time coding, adaptive modulation, and underwater acoustic communications.

HAIYAN WANG (Member, IEEE) received the B.S., M.S., and Ph.D. degrees from the School of Marine Science and Technology, Northwestern Polytechnical University (NWPU), Xi'an, China, in 1987, 1990, and 2004, respectively. He has been a Faculty Member of the NWPU since 1990 and a Professor since 2004. He teaches and conducts research with the NWPU in the areas of signal and information processing, electronics engineering, and tracking and locating of maneuvering targets. His general research interests include modern signal processing, array signal processing, underwater acoustic communications, tracking and locating of maneuvering targets, and data mining technique and its applications.